International Journal of Basic and Applied Sciences, 14 (5) (2025) 558-566

International Journal of Basic and Applied Sciences

Website: www.sciencepubco.com/index.php/IJBAS
https://doi.org/10.14419/gnbb7866
Research paper

Characteristic Analysis of Lithium Manganese Oxide Cathode Materials for Enhanced Lithium Ion Battery Performance

Prabhu S. [1] *, Vinod S. [2]*, Rudhra S. [2], Balaji M [3]

[1] *Department of Electrical and Electronics Engineering, Mohan Babu University, A. Rangampeta, Tirupati 517102, Andhra Pradesh, India*
[2] *Department of Electrical and Electronics Engineering, Jerusalem College of Engineering, Anna University, Chennai 600100, Tamil Nadu, India*
[3] *Department of Electrical and Electronics Engineering, Sri Sivasubramaniya Nadar College of Engineering, Kalavakkam 603110, Tamil Nadu, India*
**Corresponding author E-mail: vinod@jerusalemengg.ac.in*

Received: July 12, 2025, Accepted: August 26, 2025, Published: September 16, 2025

Abstract

In this work, we develop a comprehensive simulation approach to evaluate the performance of lithium-ion batteries using a $LiMn_2O_4$ (Lithium Manganese Oxide) cathode, aimed at supporting high-power electric vehicle (EV) applications. The framework integrates material selection, electrode design, and cell architecture with coupled electrochemical-thermal modeling. Electrode compositions are explicitly defined and implemented in a 3D equivalent-circuit model (RCRTable3D), further linked to thermal models to capture heat generation and dissipation. Simulations are conducted under realistic EV cycling conditions, using 1 A constant current charge–discharge cycles between 2.5 V and 3.34 V, with 10-minute rest periods at 25 °C under forced convection (100 $W/m^2 \cdot K$). This setup replicates typical vehicle operation and thermal management scenarios. Key performance indicators—temperature evolution, voltage profiles, SOC (state of charge) trends, energy throughput, and early aging signs—are analyzed to evaluate design parameter influences. Results demonstrate how integrated modeling can optimize cell performance, refining electrode structures and cycling strategies. Overall, this simulation-based study provides insights for enhancing thermal stability, efficiency, and longevity of LMO-based lithium-ion batteries in high-demand applications.

Keywords: *Lithium Manganese Oxide; Electrochemical-Thermal Modeling; State of Charge (SOC).*

1. Introduction

The growing demand for environmentally sustainable transportation has accelerated the development of lithium-ion battery technologies in electric vehicles (EVs). Among the cathode chemistries explored, lithium manganese oxide ($LiMn_2O_4$) has gained attention for its balance of performance, safety, and cost-effectiveness [1], [2]. As a cathode material, $LiMn_2O_4$ offers several advantages that align with the technical and economic requirements of mass-market EVs, particularly in urban and hybrid vehicle applications [3], [4]. $LiMn_2O_4$ features a spinel-type crystal structure that provides three-dimensional lithium-ion diffusion pathways [5], [6]. This enables rapid charge/discharge—essential for EV acceleration and regenerative braking [4], [7]. Operating at ~4.0 V versus Li/Li^+, it delivers high energy efficiency and supports extended driving range [5], [8]. Thermal stability is another key advantage of $LiMn_2O_4$-based cells. Thermally, $LiMn_2O_4$ cells have lower thermal runaway risk compared to nickel- and cobalt-rich cathodes [6], [9], improving safety under high-temperature or abusive conditions. Economically, manganese is abundant and widely distributed, unlike cobalt, which faces ethical sourcing concerns [10], [11]. This reduces costs and improves sustainability. Unlike cobalt, which is often sourced from conflict regions and associated with ethical mining concerns, manganese offers a more sustainable and less controversial supply chain. The lower material cost further enhances the viability of $LiMn_2O_4$ for large-scale adoption in automotive battery packs [12].

Despite these advantages, the long-term cycling stability of $LiMn_2O_4$ remains a challenge. However, cycling stability challenges remain. Mn^{3+} dissolution, particularly at elevated temperatures or high rates [13], [14], causes structural distortion and capacity loss. Mitigation strategies include cation doping, electrolyte additives [15], [16], and protective coatings. Moreover, the moderate specific energy of $LiMn_2O_4$ restricts its suitability for long-range EVs compared to chemistries such as NMC (Nickel Manganese Cobalt) or NCA (Nickel Cobalt Aluminum) [17]. However, for urban transport solutions—such as e-scooters, electric buses, and hybrid electric vehicles—where high power output and fast recharge capabilities are prioritized over long-range travel, $LiMn_2O_4$-based batteries remain highly competitive [18]. As advancements in cell design, electrolyte formulation, and materials engineering continue, the limitations of $LiMn_2O_4$ are

gradually being addressed [19], [20]. With its unique combination of thermal safety, high-rate capability, affordability, and sustainability [22], [23], [25], $LiMn_2O_4$ remains a promising cathode material for next-generation EVs, supporting the broader transition to clean and reliable mobility solutions. Recent advancements include dual-ion doping and novel electrolyte additives to suppress manganese dissolution (Zhang et al., 2023), and conductive MOF coatings to improve cycle life (Kim et al., 2024). Classic research by Thackeray et al. (1983) established the structural and electrochemical basis for the spinel crystal.

$LiMn_2O_4$ has lower specific energy than NMC and NCA, limiting long-range use [26 - 30]. However, for urban mobility (e-scooters, buses, hybrids), it excels due to high power output, safety, fast recharge, and low cost. Compared to NMC/NCA, it offers superior thermal stability and intrinsic safety, making it ideal where safety and cost outweigh maximum range.

2. Method

LiMn2O4 serves as a promising cathode material for lithium-ion batteries due to its effectiveness and low environmental impact. Effective battery modeling of LiMn2O4 focuses on its electrochemical behavior, particularly the intercalation of lithium ions, which is crucial for understanding charge and discharge kinetics. Additionally, thermal management is essential, as temperature fluctuations can significantly influence battery performance and safety. Models often incorporate thermal dynamics to predict temperature variations during operation, which can affect overall battery life. Furthermore, performance degradation mechanisms, such as structural changes in the cathode and electrolyte breakdown, are critical areas of study. Understanding these degradation processes is vital for developing strategies to minimize capacity loss and extend battery lifespan. Researchers employ various modeling techniques, including reduced-order and full-order electrochemical models, to simulate the behavior of LiMn2O4 batteries under different conditions, aiding in the optimization of battery design and enhancing the accuracy of state of charge (SOC) estimations.

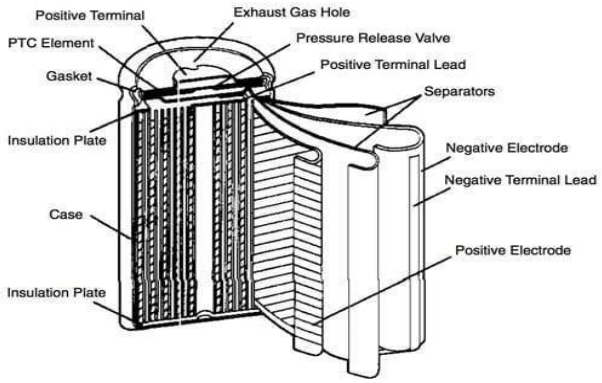

Fig. 2.1: Internal Structure of a Cylindrical $LiMn_2O_4$ Cell.

Figure 2.1 illustrates that LiMn2O4 is primarily used as a cathode material in lithium-ion batteries, but its role as a negative electrode is less common. When utilized in this capacity, it can provide benefits such as improved safety and thermal stability. LiMn2O4 features a spinel structure that allows for efficient lithium-ion intercalation and deintercalation, contributing to stable cycling performance. However, its lower theoretical capacity compared to traditional anode materials like graphite limits its application as a negative electrode. Research continues to explore its potential in hybrid configurations, aiming to enhance overall battery performance and longevity while maintaining safety.

2.1. Selected IET Model

This research presents the RCRTable3D IET model, which uses a resistance-capacitance-resistance (RCR) network to simulate electrochemical processes such as charge transport and diffusion. It integrates 3D spatial resolution to capture variations in temperature, voltage, and current. Using SOC- and temperature-dependent resistance/capacitance tables, it models internal heating, voltage behavior, and thermal regulation for high-power EV applications.

3. Electrode Materials, Properties, and Cell Report

3.1. Defined Electrode Materials and Properties

Table 3.1: Positive and Negative Electrode Properties of $Limn_2O_4$ Cell

Component	Material Name	Positive Electrode Weight (g)	Positive Electrode Volume (cm^3)	Negative Electrode Weight (g)	Negative Electrode Volume (cm^3)
Formulation	Spinel Mn2O4	3.520	0.545	-	-
Formulation	PVDF	0.074	0.028	-	-
Formulation	Graphite2	0.111	0.035	-	-
Collector	Al Foil (30um)	1.577	0.584	-	-
Tab	Aluminium (1100)	0.0106	0.0039	-	-
Tape	Polyimide	0.0067	0.0045	-	-
Formulation	Graphitefade	-	-	2.187	0.744
Formulation	CMC	-	-	0.165	0.123
Collector	Cu Foil (18um)	-	-	3.520	0.395
Tab	Nickel 270	-	-	0.024	0.0027
Tape	Polyimide	-	-	0.007	0.0046

Table III.It shows the electrode materials table, which summarizes the composition of both positive and negative electrodes, listing essential components such as active materials, binders, collectors, and tabs. The positive electrode primarily consists of spinel Mn_2O_4 as the

active material, while the negative electrode uses graphite-based formulations. The weight and volume of each component contribute to the overall cell performance, influencing energy capacity, thermal stability, and mechanical integrity.

3.2. LiMn2O4 Cell Report

Table III.II shows the essential information regarding the battery's performance and structural attributes. It includes key parameters such as voltage, capacity, energy, and energy density, which define the battery's power output. The material cost is an important metric in determining economic feasibility, while electrolyte and separator properties impact ionic conductivity and battery lifespan. Heat capacity at 25°C indicates the thermal stability of the cell, which is crucial in preventing overheating during charge-discharge cycles.

Table 3.2: Cell Properties of Limn2o4 Cell

Property	Value
State of Charge (%)	100.00
Voltage (V)	3.24
Capacity (Ah)	0.0033
Energy (Wh)	0.0106
Energy Density (Wh/kg)	0.015
Energy Density (Wh/liter)	0.077
Weight (g)	722.647
Volume (cm^3)	138.160
Materials Cost ($)	3.12
Active Area (m^2)	0.037
Unit Capacity (mAh/cm^2)	0.379
C/A Ratio (mAh/mAh)	0.543
Electrolyte Mass (g)	610.354
Electrolyte Volume (cm^3)	471.568
Separator Area (m^2)	0.056
Heat Capacity @25°C (J/g·K)	0.992

The table III.III shows a comparative analysis of the positive and negative electrodes, focusing on structural and electrochemical parameters. The average voltage and stoichiometry at formation determine the battery's voltage stability and reaction efficiency. Coating thickness, porosity, and weight affect the electrode's ability to hold active material and influence cycle life. Loading values indicate the material deposition per unit area, which directly impacts energy capacity and charge retention.

Table 3.3: Computed Electrode Properties of Limn2o4 Cell

Property	Positive Value	Negative Value
Average Voltage (V)	3.33	0.093
Stoichiometry at Formation	0.657	0.521
Unit Capacity (mAh/cm^2)	0.379	1.059
Thickness (w/collector) (µm)	104.911	97.921
Coating Porosity (%)	33.4	25.1
Coated Length (cm)	65.419	67.919
Coating Thickness (µm)	37.456	39.961
Coating Weight (g)	3.705	2.351
Total Length (cm)	34.760	38.459
Loading (mg/cm^2)	20.226	12.148

4. Simulation Setup and Simulation Analysis

A simulation setup was established to investigate the electrochemical performance of LiMn2O4 as a cathode material in lithium-ion batteries, as shown in flowchart 4.1. The flowchart represents the simulation setup for the $LiMn_2O_4$-based cell, outlining the charging and discharging cycle. The process starts with a discharge phase at 1A until the voltage reaches 2.5V. After this, the cell undergoes a 10-minute rest period, ensuring stabilization before charging. The charging step also occurs at 1A, with the voltage increasing until it reaches 3.34V. Another 10-minute rest phase follows to allow.

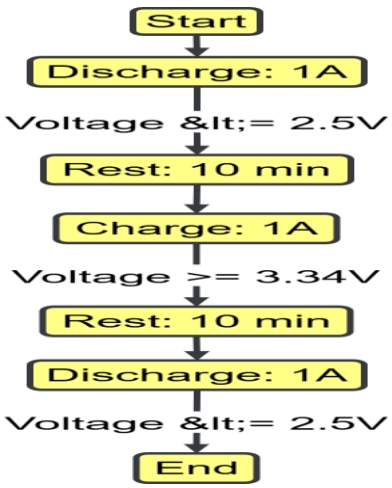

Fig. 4.1: Simulation Set Up of LiMn2O4 Cell.

Equilibrium. The process concludes with a second discharge cycle at 1A, again stopping at 2.5V, after which the simulation ends. This structured cycling helps evaluate the cell's performance under controlled conditions, ensuring accurate assessment of charge retention and degradation behavior.

5. Results and Discussion

5.1. Thermal Stability Analysis

5.1.1. Temperature vs. Time (test (hr))

Figure 5.1 shows the temperature over the cycler condition time duration in hours. The battery cell starts at an initial temperature of 25°C, gradually increasing to a peak of 45.84°C during operation. This steady temperature rise indicates that while heat is being generated, it is also dissipated effectively, preventing sudden overheating. The balanced heat transfer ensures stable operation, but prolonged use at elevated temperatures may accelerate degradation. Implementing appropriate cooling methods, such as air or liquid cooling, can help maintain optimal thermal performance and extend battery life.

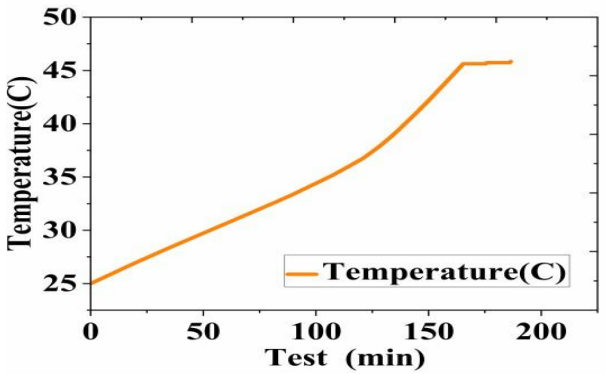

Fig. 5.1: $LiMn_2O_4$ Cell Temperature Profile of the Battery Over Time.

5.1.2. Heat generation vs. time (test (hr))

Figure 4.5 shows the Heat Generation in the Battery System Over the cycler condition time duration in hours. The heat generated by the cell increases progressively throughout discharge, reaching a peak of 0.404 W. This trend is primarily attributed to rising internal resistance and Joule heating effects. A controlled increase in heat generation suggests that the electrochemical processes are functioning within expected parameters. However, excessive heat buildup over time could impact efficiency.

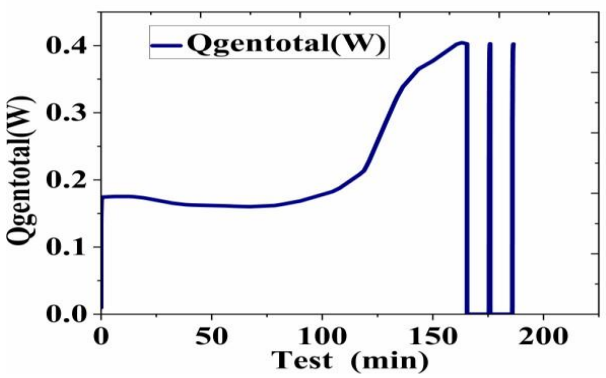

Fig. 5.2: $LiMn_2O_4$ Cell Heat Generation in the Battery System Over Time.

And durability. Regular monitoring of heat generation helps in optimizing thermal management strategies to maintain battery health.

5.1.3. Heat balance vs. time (test (hr))

The heat balance distribution of the designed LiMn2O4 cell throughout the test is shown in Figure 5. .3. Initially, heat accumulation remains minimal but gradually increases as cycling progresses. A stable heat balance suggests an effective thermal management system that prevents excessive temperature buildup.

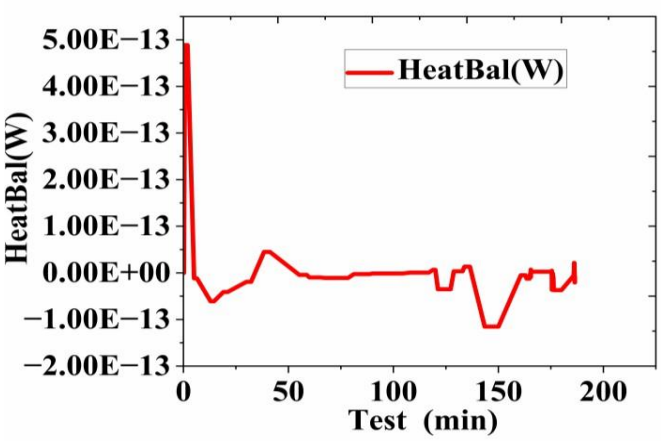

Fig. 5.3: $LiMn_2O_4$ Cell Heat Balance Distribution Throughout the Testing Period.

5.2. State of Charge (soc) and Energy Efficiency

5.2.1. SOC vs. time (test (hr))

Figure 5.4 graphically represents the state of charge (SOC) throughout the test period. The state of charge exhibits a steady decline from 99.99% to a minimum of 4.92% as the battery undergoes discharge. This non-linear decline reflects the nature of lithium-ion electrochemical reactions, maintaining performance stability for most of the cycle. Ensuring proper SOC management helps prevent deep discharges, which can accelerate aging and reduce efficiency. A well-regulated SOC profile ensures longevity and reliable operation across multiple cycles.

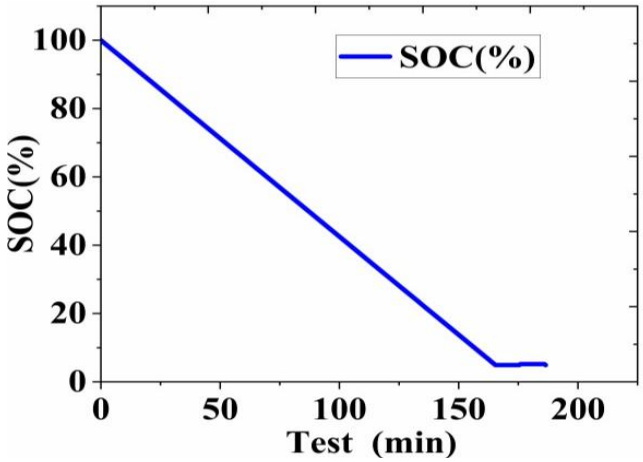

Fig. 5.4: $LiMn_2O_4$ Cell State of Charge (SOC) Profile Over Time.

5.2.2. Cumulative capacity and energy vs. time (test (hr))

The gradual increase in cumulative capacity throughput throughout the test is illustrated in Figure 5.5. The battery accumulates a total capacity of 2.76 Ah, demonstrating stable charge retention over time. While a minor decline in capacity is observed, it aligns with expected degradation patterns seen in lithium-ion cells. Monitoring cumulative capacity trends can provide insights into aging effects, allowing for early detection of potential performance issues. Proper charge-discharge cycling and optimized charging methods can help sustain capacity retention over prolonged usage.

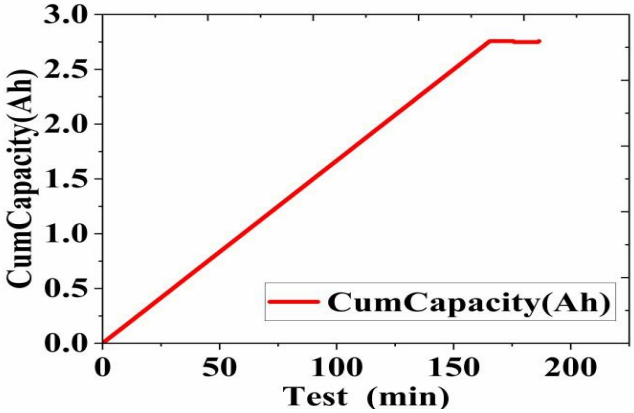

Fig. 5.5: $LiMn_2O_4$ Cell Cumulative Capacity Throughput Over Time.

5.3. Voltage Response and Capacity Retention

5.3.1. Voltage vs. time (test duration)

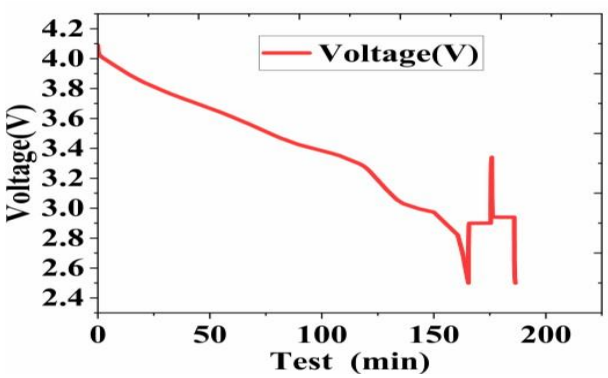

Fig. 5.6: $LiMn_2O_4$ Cell Battery Voltage Over Time.

The voltage profile starts at 4.09V and gradually declines to approximately 2.50V during discharge. This trend follows a typical lithium-ion discharge curve, where a stable plateau is maintained before a sharp drop-off at lower SOC levels. The presence of a consistent voltage plateau suggests efficient electrochemical reactions, but a significant drop at lower SOC may indicate increasing internal resistance. Avoiding over-discharge can help preserve cell longevity, and overall efficiency is shown in Figure 5.6

5.3.2. Cycle capacity vs. cycle number (test duration)

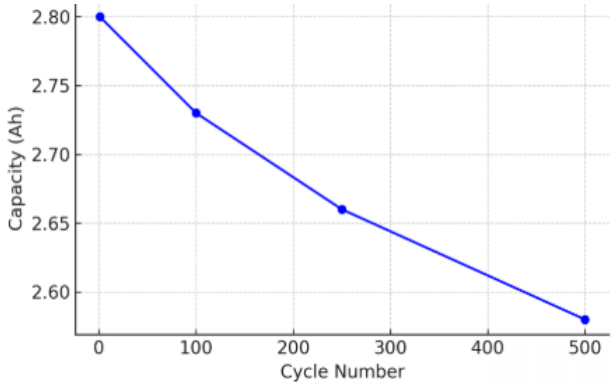

Fig. 5.7: $LiMn_2O_4$ Cell Cycle Capacity Over Test duration.

Figure 5.7 shows cycle capacity trends. In this study, the initial capacity was 2.76 Ah, declining to 2.60 Ah after 500 cycles (~5.8% fade). This decline is due to normal aging effects such as electrode wear and side reactions.

5.3.3. Cycle energy vs. cycle number (test duration)

Figure 5.8 shows the average cycle energy. It started at 9.50 Wh and decreased to 8.90 Wh after 50 cycles (93.7% retention). This loss correlates with internal resistance growth and efficiency reduction.

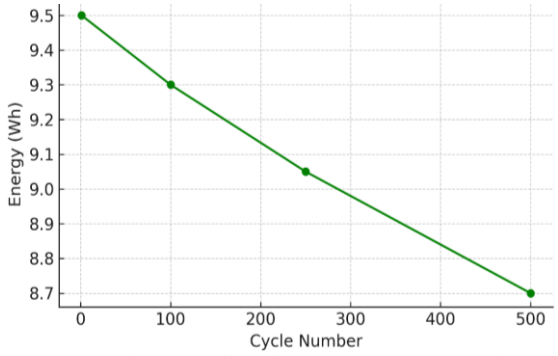

Fig. 5.8: $LiMn_2O_4$ Cell Cycle Energy Over Test Duration.

5.3.4. Open circuit voltage (OCV) vs. state of charge (SOC)

The linear relationship between Open Circuit Voltage (OCV) and State of Charge (SOC) is highlighted in Figure 5.9. The OCV follows a predictable trend, starting at 4.09V when fully charged and gradually decreasing with SOC. A well-defined OCV-SOC relationship ensures accurate battery management, allowing for precise charge estimations. Monitoring this behavior over time helps detect potential aging effects and deviations in electrochemical behavior, which could impact performance.

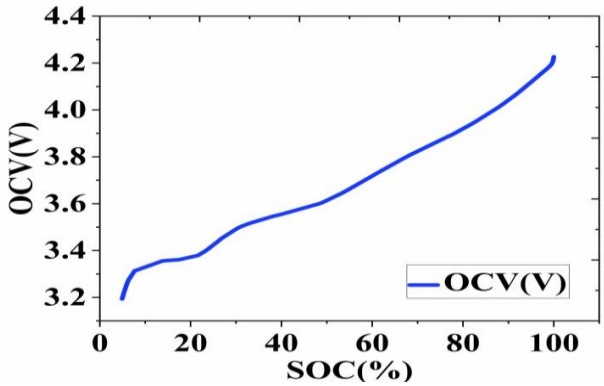

Fig. 5.9: $LiMn_2O_4$ Cell Open Circuit Voltage in Relation to SOC.

5.3.5. Voltage vs. state of charge (SOC)

Figure 5.10 depicts a graphical representation of the relation between SOC and Voltage. The voltage-SOC profile exhibits a stable discharge trend, particularly between 40% and 80% SOC.

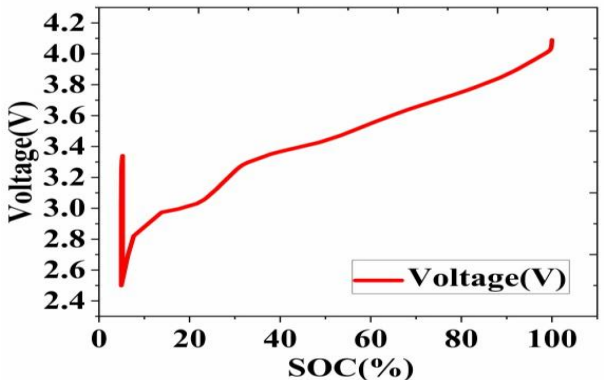

Fig. 5.10: $LiMn_2O_4$ Cell Battery Voltage as a Function of SOC.

This range represents efficient lithium-ion intercalation and extraction, which is essential for maintaining performance consistency. Any significant deviation from this pattern may indicate aging effects, such as electrode degradation or lithium inventory loss, which could impact capacity and efficiency.

5.4. Thermal and Electrical Properties

5.4.1. Thermal conductivity and heat transfer vs. time (test (hr))

The steady heat transfer coefficient in W/m²-K throughout the test period. The heat transfer coefficient remains stable at approximately 100 W/m²-K, indicating efficient thermal dissipation. This stability prevents localized overheating, ensuring safe operation is inferred from Figure 5.11. Any significant variations in heat transfer could suggest changes in material conductivity or potential cooling inefficiencies, requiring further analysis and adjustments.

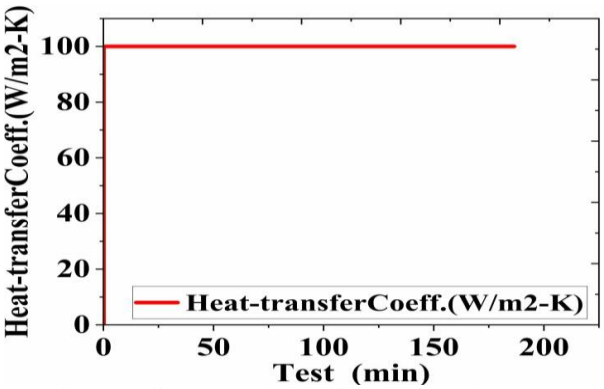

Fig. 5.11: $Limn_2O_4$ Cell Heat Transfer Coefficient(W/M2-K) Over Test Duration.

5.4.2. Ohmic resistance vs. time (test (hr))

The ohmic resistance behavior throughout the Test period after an initial increase is clearly illustrated in Figure 5.12. The ohmic resistance remains relatively low, peaking at 0.0046 Ω-m². A gradual increase in resistance over time is expected due to electrode wear and electrolyte aging. Maintaining low internal resistance is crucial for preserving efficiency and minimizing energy losses. Proper material selection and optimized electrode design can help manage resistance growth over prolonged operation.

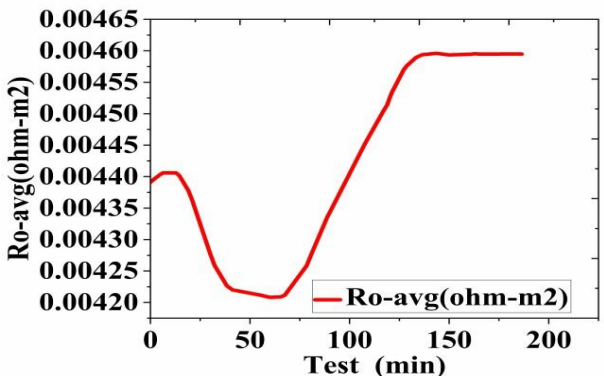

Fig. 5.12: $LiMn_2O_4$ Cell Average Ohmic Resistance (ohm-m²) Over Test Duration.

5.4.3. Power output vs. time(hr)

The power output reaches a peak of 4.09W and gradually declines as voltage decreases during discharge is shown in Figure 5.13 graphically represents the Power output of the cell throughout the test period.

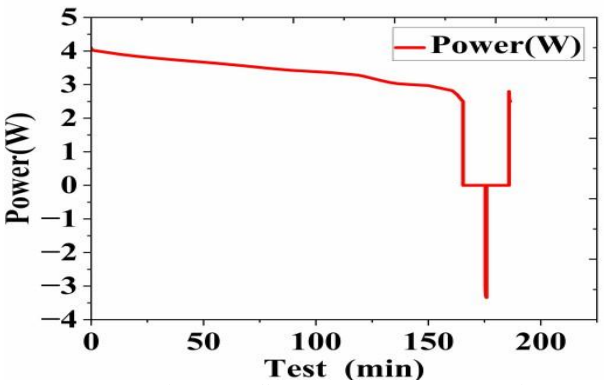

Fig. 5.13: $LiMn_2O_4$ Cell Power (W) Over Test Duration.

This trend suggests stable power delivery, which is essential for applications requiring consistent energy output. Ensuring power stability enhances performance reliability, particularly in high-demand applications like electric vehicles and portable electronics.

6. Conclusion

Thermal and electrochemical evaluation of the $LiMn_2O_4$ cell shows reliable operation with minimal thermal stress. The temperature rose from 25 °C to ~45.8 °C with controlled heat generation. SOC declined predictably, delivering 2.76 Ah and 9.50 Wh. A stable 4.09–2.50 V range and gradual capacity fade indicate predictable aging. Proper thermal and charge management remains essential for maximizing performance. Looking ahead, research could explore hybrid cathode–anode combinations that strike the right balance between higher energy density and longer cycle life. Equally important is the need for scalable methods to recycle and regenerate spent $LiMn_2O_4$ cells, ensuring sustainable use of resources. Another promising direction is the use of multi-layer protective coatings together with advanced electrolyte additives, which could help reduce manganese dissolution and improve the thermal stability of the cells, ultimately making lithium manganese oxide batteries safer and more reliable.

References

[1] Nyamaa O., Jeong H.-M., Kang G.-H., Kim J.-S., Goo K.-M., Baek I.-G., Yang J.-H., Nam T.-H., Noh J.-P., "Enhanced $LiMn_2O_4$ cathode performance through synergistic cation and anion substitution", Journal of Materials Advances, issue 7, 2872–2887, 2024, https://doi.org/10.1039/D3MA01187A.

[2] Pan B., Zhang H., Weng Y. "Improvement of electrochemical performance of spherical spinel $LiMn_2O_4$ coated with Al-doped ZnO (AZO)", International Journal of Ionics-the science and technology of Ionic motion, Volume 30, pages 1359–1372,2024. link.springer.com+1en.wikipedia.org+1. https://doi.org/10.1007/s11581-024-05403-w.

[3] Liang P., Li Y., Xiao X., Fan S., Ma J., Liu J., Dong Y., Zong Y., Xu G., Yang L., "Large-scale synthesis of $LiMn_2O_4$ via rheology-assisted solid-phase method with citric acid", New Journal od chemistry ,issue 17, 7911–7920, 2024, https://doi.org/10.1039/D4NJ00767K.

[4] Yurilshmatok, Hanna Potapenka, Sviatoslav Kirillov, "Optimal design of $LiMn_2O_4$ for high-rate applications by citric acid aided route and microwave heating", Journal of electro chemical science and engineering, 14(3), 369–382, 2024, https://doi.org/10.5599/jese.2253.

[5] Kong J., Guo H., Li Y., Gong M., Lin X., Zhang L., Wang D, "Highly improved aqueous Zn‖$LiMn_2O_4$ hybrid-ion batteries using PEG and manganese sulfate additives ", Sustainable energy & fuels, issue 4, 826–836, 2024, https://doi.org/10.1039/D3SE01295F.

[6] Zhang G., Zhang P., Kong S., Jin B., "Spinel $LiMn_2O_4$ as electrocatalyst toward solid-state zinc–air batteries", Journal of Catalysts, 13(5), 860, 2023, https://doi.org/10.3390/catal13050860.

[7] Urbi Pal, Binayak Roy, Meisam Hasanpoor, et al, "Developing a high-performing spinel $LiMn_2O_4$ cathode with unique morphology, fast cycling and scaled manufacture, Journal of Batteries & Supercaps, volume 7, issue 6, 1-9 2024, https://doi.org/10.1002/batt.202400072.

[8] Yu Q., Li P., Guo Q. "Synthesis and properties of $LiMn_2O_4$ cathode material for lithium-ion batteries", International Research Journal of Pure Applied Chemistry., Vol 25, issue 3, 14-21, 2024, https://doi.org/10.9734/irjpac/2024/v25i3852.

[9] Gonzalez Rosillo J.C., Guc M., Liedke M.O., Butterling M., Attallah A.G., Hirschmann E., Wagner A., Izquierdo-Roca V., Baiutti F., Morata A., Tarancon A., "Insights into $LiMn_2O_4$ cathode stability in aqueous electrolyte", Chemistry of Materials, 36(12), 6144–6153, 2024, https://doi.org/10.1021/acs.chemmater.4c00888.
[10] He Z.Y., Ross N., Willenberg S., Juqu T., Carleschi E., Doyle B.P., "Boosting $LiMn_2O_4$ diffusion & stability via Fe/Mg doping and MWCNT microstructure modulation", Journal of Nanotechnology, 2024, Article 7020995, https://doi.org/10.1155/2024/7020995.
[11] Kim E., Lee J., Park J., Nam K.W., "Conductive MOF coating for suppressing Mn dissolution in $LiMn_2O_4$ for long-life LIBs", SSRN, 2024, https://doi.org/10.2139/ssrn.4799030.
[12] He Y.-L., Gu Y.-J., Chen Z.-L., Ma X.-Y., Wu F.-Z., Dai X.-Y., "Improved $LiMn_2O_4$ derived from MOFs by organic ligands", *New Journal of Chemistry*, 47, 14068–14077, 2023, https://doi.org/10.1039/D3NJ02345A.
[13] Xiao X., Wang L., Wu Y., Song Y., Chen Z., He X., "Cathode regeneration and upcycling of spent LIBs: toward sustainability", *Energy & Environmental Science*, 16(7), 2856–2868, 2023, https://doi.org/10.1039/D3EE00746D.
[14] Yang T., Luo D., Yu A., Chen Z., et al., "Enabling closed loop recycling of spent LIBs: direct cathode regeneration", *Advanced Materials*, 35(36), 2023, https://doi.org/10.1002/adma.202203218.
[15] MacKenzie et al., "Direct conversion of waste battery cathodes to high-volume capacity anodes", *Advanced Energy Materials*, 13(22), 2023, https://doi.org/10.1002/aenm.202300596.
[16] Min H., Peng Z., Duan X., Teng L., Li J., Liu W., "Selective recovery of lithium from spent LIBs via emission-free sulfation", *Process Safety and Environmental Protection*, 177, 1035–1044, 2023, https://doi.org/10.1016/j.psep.2023.05.014.
[17] Fang W., Yan L., An Z., Xia H., "Study on different mass ratios of $LiMn_2O_4$//AC lithium-ion capacitor", *Research Square*, 2023.
[18] Abdelaal M.M., Alkhedher M., "Dual optimization of $LiFePO_4$ cathode using manganese substitution & PEDOT:PSS coating", *Electrochimica Acta*, 506, 145050, 2024, https://doi.org/10.1016/j.electacta.2024.145050.
[19] Nagappan N., Priyanga G.S., Thomas T., "Insights into alloying elements' impact on predicted battery voltage in metal ion batteries", *Journal of* Energy Storage, 103, 114412, 2024, https://doi.org/10.1016/j.est.2024.114412.
[20] Gao Y., Li J., Hua Y., Yang Q., et al., "Recent advances of metal fluoride cathode materials for LIBs", Materials Futures, 3(3), 032101, 2024, https://doi.org/10.1088/2752-5724/ad4572.
[21] Sivasamy S., Vinod S., Balaji M., Rudhra S., Prabhu S., "Electrochemical and thermal characterization of the Li-NCM NM3100 cell for EV applications", International Journal of Environmental Sciences, 11(4), 947–961, 2025.
[22] Prabhu S., Vinod S., Rudhra S., Balaji M., "Green evaluation of Lithium Iron Phosphate (LFP) batteries: Environmental consequences of electrochemical, thermal, and aging factors", International Journal of Environmental Sciences, 11(3), 957–970, 2025.
[23] Satish Kumar S., Pramila V., Rudhra S., Vinod S., Lakshmi D., "Enhancing demand response and energy management in multi-microgrid systems with renewable energy sources", *Renewable Energy*, 253, 2025, https://doi.org/10.1016/j.renene.2022.12.105.
[24] Vinod S., Balaji M., Rudhra S., Prabhu S., "Solar powered DC arc welding machine – an initiative towards efficient and sustainable energy", *Journal of Environmental Protection and Ecology*, 24(3), 888–894, 2023.
[25] Prabhu S., Vinod S., Rudhra S., Balaji M., "Model-Based Evaluation of Li–NCM Battery Performance for Environmentally Resilient Energy Systems", International Journal of Environmental Sciences, 11(5), 676–688, 2025. https://doi.org/10.1109/ICAEECI58247.2023.10370780.
[26] Madhaiyan, V., Murugesan, R., Sengottaiyan, S., Muniyan, V., Vijayakumar, A., & Sundaramoorthy, P. (2023). Analysis of performance for multilevel inverters utilizing different pulse width modulation techniques. Proceedings of the First International Conference on Advances in Electrical, Electronics and Computational Intelligence (ICAEECI), Tiruchengode, India, 1–7. https://doi.org/10.1109/ICAEECI58247.2023.10370780.
[27] Prabhu, S., & Balaji, M. (2022). Performance analysis of permanent magnet assisted outer rotor switched reluctance motor with non-oriented laminating material for electric transportation systems. Proceedings of the IEEE 2nd International Conference on Sustainable Energy and Future Electric Transportation (SeFeT), Hyderabad, India, 1–6. https://doi.org/10.1109/SeFeT55524.2022.9909350.
[28] Sivasamy, S., Sundaramoorthy, P., & Beno, M. (2023). A comprehensive investigation of outer rotor permanent magnet switched reluctance motor for enhanced performance in electric vehicles. IEEE Canadian Journal of Electrical and Computer Engineering, 46(4), 342–347. https://doi.org/10.1109/ICJECE.2023.3316261.
[29] Prabhu, S., Arun, V., Balaji, M., Kalaimagal, V., Manikandan, A., & Chandrasekar, V. (2023). Electromagnetic analysis on interior permanent magnet motor for electrified transportation systems. Proceedings of the 9th International Conference on Electrical Energy Systems (ICEES), Chennai, India, 163–168. https://doi.org/10.1109/ICEES57979.2023.10110040.
[30] Madhaiyan, V., Murugesan, R., Arun, V., & Prabhu, S. (2023). Nine switch dual input 9-level inverter (NSDI9LI) with inherent AC voltage generation ability. Proceedings of the First International Conference on Advances in Electrical, Electronics and Computational Intelligence (ICAEECI), Tiruchengode, India, 1–5. https://doi.org/10.1109/ICAEECI58247.2023.10370814.